JOURNAL OF SOLID STATE CHEMISTRY 98, 40–47 (1992)

The Synthesis, Crystal Structure and Electrical Properties of $[Fe_xMn_{1-x}]Ta(O_2)O_2$ with $x \approx 0.3$

DENG SHUIQUAN,* AND ZHUANG HONGHUI

Fujian Institute of Research on the Structure of Matter, Chinese Academy of Sciences, Fuzhou, Fujian 350002, People's Republic of China

AND HUANG JINLING

Fuzhou University, Fujian, People's Republic of China

Received May 16, 1991; in revised form October 18, 1991

The new layered compound $[Fe_xMn_{1-x}]Ta(O_2)O_2$ ($x \approx 0.3$) has been prepared and structurally characterized. This compound crystallizes in orthohombic system (C_{2v}^2 – $Pmc2_1$), a = 4.726(1), b = 5.697(2), c = 4.963(1) Å with two formula units in the cell. The structure contains Ta and M atoms in unusual trigonal prismatic environments with the Ta–O distances ranging from 1.74(2) to 1.995(9) Å, and the M–O distances from 2.10(2) to 2.24(2) Å. Each M site is statistically occupied by about 30% Fe atoms and 70% of Mn atoms ($M \approx 0.3$ Fe + 0.7 Mn). Metrical details are discussed. Results of electrical resistivity measurements on the new material indicate the saturated semiconductor behavior along the c-axis.

Introduction

The structures (*1*) of the tantalum oxides are very complex. TaO has the NaCl structure, while TaO_2 has the rutile structure. In marked contrast to TaO and TaO_2 is the complexity of Ta_2O_5; there are at least two distinct forms of Ta_2O_5, with a transition point at 1360°C. The structure of the low temperature form is composed of chains built of octahedral and/or pentagonal bipyramidal groups sharing two opposite vertices, these chains being joined by vertex- or edge-sharing to give the 3D structure; the high temperature form of Ta_2O_5 has the rutile structure.

We have recently studied the oxides of tantalum and discovered a new compound $[Fe_xMn_{1-x}]Ta(O_2)O_2$ ($x \approx 0.3$). The results showed that the structure of $[Fe_{0.3}Mn_{0.7}]Ta(O_2)O_2$ is significantly different from the above ones.

Experimental

A combination of powders of Fe_2O_3 (99.8%, 0.028 g), MnO_2 (99.9%, 0.031 g), Ta_2O_5 (99.999%, 0.221 g), and an excess of Fe (99.8%, 0.010 g) and Mn (99.9%, 0.010 g) was thoroughly ground under an N_2 atmosphere and then pressed into a pellet. The pellet was loaded in a silica tube that was then evacuated to $\sim 10^{-6}$ Torr. The tube was sealed and placed in a tube furnace that was

* To whom correspondence should be addressed.

0022-4596/92 $5.00

heated at 900°C for 1 week. After radiative cooling, the tube was removed from the furnace and the contents were thoroughly ground under an N_2 atmosphere. The pellet of the samples was then placed in a fresh silica tube. After being evacuated and sealed, the tube was heated at 1000°C for 72 hr. This procedure of grinding and heating (1000°C) was repeated several times in order to obtain the homogeneous phase. The prepared quaternary compound was then used as source material to be transported by iodine. After being evacuated to $\sim 10^{-6}$ Torr and sealed, the transport tube was kept in the temperature gradient of 1100 ~ 1180°C for 2 weeks, with the sample at the higher temperature end. After cooling at 20°C/hr., the black powder and prism-shaped crystals were produced at the cold end of the tube. Crystals of 0.032 g picked out from the reaction tube were analyzed on a Perkin–Elmer 306 Atomic-Absorption spectrophotometer. The vacuum extraction technique (*2, 3*) for determination of gaseous elements from solid metals was used to determine the oxygen content. Anal. calcd. for $[Fe_{0.3}Mn_{0.7}]Ta(O_2)O_2$: Fe, 5.6; Mn, 12.8; Ta, 60.3; O, 21.3. Found: Fe, 5.9; Mn, 12.6; Ta, 62.5; O, 22.7. The density was measured by a micropycnometer method in benzene. The observed density is 7.4(2) g/cm^3. IR spectra between 200–1200 cm^{-1} were obtained from KBr pellets on a Perkin–Elmer 577 Grating Infrared Spectrophotometer. IR data (cm^{-1}): 872(s), 500–800(s) broad band, 250–350(s) broad band.

Resistivity Measurements

Resistivities were measured on two single crystals of the sample by a four-probe technique (*4, 5*). Electrical contacts of four silver wires (0.11 mm) on the surface (001) of the first crystal (1.00 mm × 0.80 mm × 0.70 mm), and (100) of the second crystal (1.10 mm × 0.90 mm × 0.62 mm) were made with silver paint. Then the sample crystal on a crystal holder, appropriately shielded in a capillary tube from the gas currents, was placed in a Dewar flask. Boil-off gas from a liquid N_2 or He reservoir was channeled through the Dewar and over the crystal holder. The crystal temperature was measured by a 2.1 atom% CoAu vs copper thermocouple positioned within 2–3 mm of the enclosed crystal. The sample temperature was varied by controlling the cryogenic gas boil-off. Cooling and warming rates were maintained in the vicinity of 1–2 K/min. The three principal components of the resistivity tensor as a function of the temperature were measured. Our results show that the material is very anisotropic with $\rho_a, \rho_b \gg \rho_c$. Temperature-dependent resistivity ρ_c is shown in Fig. 5 below.

Structure Determination

The unit cell parameters were determined from least-squares refinements of 20 reflections in the range $40° \leq 2\theta$ (Mo$K\alpha$) $\leq 55°$ with a crystal that had been automatically centered on a MSC/Rikagu diffractometer. A total of 523 independent reflections were collected within the range of $2° < 2\theta < 80°$, in $\omega - 2\theta$ scan mode, of which 457 reflections with $I > 3\sigma(I)$ were considered to be observed. Lorentz-polarization and anisotropic decay corrections were applied. From the systematic absences of $h0l$, $l = 2n$, and the subsequent least-squares refinement, the space group was determined to be $Pmc2_1$. The crystal data and other relevant data collection parameters are given in Table I.

The structure was solved using the patterson method which revealed the position of the Ta atom. The remaining atoms were located in succeeding difference Fourier synthesis. Composition of the crystal was established through the inclusion of statistical distribution of Fe and Mn in the final of full matrix least-squares refinements on F_o. As a result of the small difference between

TABLE I

CRYSTAL DATA AND DATA COLLECTION PARAMETERS

Formula	$[Fe_{0.3}Mn_{0.7}]Ta(O_2)O_2$	Crystal Dimension, mm	0.40 × 0.20 × 0.30
M_r	300.25	Scan type	$\omega - 2\theta$
Crystal system	orthorhombic	Scan width ( )	1.22 + 0.35tgθ
Space group	$Pmc2_1$	Scan rate (deg/min)	16 (in ω)
a (Å)	4.726(1)	Corrections	Lorentz-polarization
b (Å)	5.697(2)	linear decay	(from 0.972 to 1.000)
c (Å)	4.963(1)	Extinction	(coefficient = 0.0000018)
V (Å^3)	133.63(6)	2θ range (deg)	2–80
Z	2	hkl range	h = −8–0, k = 0–10, l = 0–8
D_x (g cm^{-3})	7.46 g/cm^3	No. of refl. measured	523
D_m (g cm^{-3})	7.4(2) g/cm^3	No. of refl. unique	523
μ	249.5 cm^{-1}	No. of refl. refined	457 with $I > 3.0\sigma(I)$
Radiation	Mo$K\alpha$ (λ = 0.71069 Å)	No. of refl. standard	3
Monochromator	graphite	Quality of fit (GOF)	1.71
F(000)	310	Largest shift/esd.	0.01
R	0.038	Minimization function	$\Sigma[w(\|F_o\| - \|F_c\|)^2]$
R_w	0.041	Weight scheme	7 Ref. (*23*)
Crystal color	black	Highest residue (e/A^3)	1.58
Crystal shape	prism	Lowest residue (e/A^3)	0.47

the scattering powers of Fe and Mn, the refinement is not sensitive to the change of occupancies of Fe and Mn, so we take the result of atomic absorption analysis to determine the occupancies of Fe and Mn. The final composition of the material was written as $[Fe_xMn_{1-x}]Ta(O_2)O_2$ with $x \approx 0.3$. The final $R = 0.038$, $R_w = 0.041$. An analysis of $\Sigma w(|F_o| - |F_c|)^2$ as a function of sin θ/λ, $|F_o|$, and Miller indices revealed no unusual trends. Final positional parameters and Anisotropic thermal parameters are given in Table II and Table III, respectively.

TABLE II

POSITIONAL PARAMETERS AND THEIR ESTIMATED STANDARD DEVIATIONS

Atom	X	Y	Z	B(Å^2)
Ta	0.5000(0)	0.1803(2)	0.0000(0)	0.320(7)
M	0.0000(0)	0.3277(4)	−0.5157(7)	0.32(3)
O(1)	0.3334(1)	0.107(2)	−0.335(2)	1.28(9)
O(2)	0.259(2)	0.374(2)	0.145(2)	1.0(1)

Note. $M \approx 0.3$ Fe + 0.7 Mn.

Results and Discussion

The results indicate that the compound $[Fe_{0.3}Mn_{0.7}]Ta(O_2)O_2$ forms a new layered-type structure of Ta–O chemistry with the layers nearly parallel to the plane (100). The structure is realized by stacking the layers along the direction [100] in a pseudo-closest-packed manner (· · · AbAcAbAc · · ·). Projection of three layers (bAc) onto the (100) plane is given in Fig. 1, where b represents the Ta layer, A represents the O layer, and c represents the M layer. From Fig. 1 we can see that in the tantalum layer the Ta atoms form a series of collocated zigzag chains along the c-axis. The distance between two nearest-neighbor Ta atoms in a chain is 3.22 Å, therefore there exists some Ta · · · Ta interaction in the chain. Figure 1 also shows that M atoms are inserted in the vacant trigonal column along the a-axis.

Figure 2 is a perspective view of the structure and gives a labeling scheme. From Fig. 2 we can see clearly that the structure is formed by stacking the oxygen and metal layers along the a-axis. The plots of the co-

TABLE III

GENERAL DISPLACEMENT OF PARAMETERS EXPRESSIONS—B'S FOR CRYSTAL OF $[Fe_{0.3}Mn_{0.7}]Ta(O_2)O_2$

Name	$B(1,1)$	$B(2,2)$	$B(3,3)$	$B(1,2)$	$B(1,3)$	$B(2,3)$	Beqv
Ta	0.26(1)	0.27(1)	0.43(1)	0	0	0.07(4)	0.320(7)
M	0.32(6)	0.57(6)	0.08(7)	0	0	−0.18(7)	0.32(3)
O(1)	2.00(2)	0.5(2)	1.3(2)	0.1(3)	−0.1(2)	−0.1(2)	1.28(9)
O(2)	1.6(3)	0.4(2)	1.0(2)	0.0(2)	−0.8(2)	−0.2(2)	1.0(1)

Note. The form of the anisotropic displacement parameters is $\exp[-0.25\{h^2a^2B(1,1) + k^2b^2B(2,2) + l^2c^2B(3,3) + 2hkabB(1,2) + 2hlacB(1,3) + 2klbcB(2,3)\}]$, where *a*, *b*, *c* are reciprocal lattice constants.

ordination polyhedrons of Ta and *M* appear in Fig. 3 and Fig. 4. Both of them may be viewed as deformed trigonal prisms; the former is composed of two $(O_2)^{2-}$ ions and two O^{2-} ions, the latter consists of four O^{2-} and two terminal O ions from two different $(O_2)^{2-}$ ions.

Metrical details appear in Table IV. The atomic and ionic radii of the tantalum are almost the same as those of niobium (*6*) (r_{Ta} = 1.46 Å, r_{Nb} = 1.45 Å, r_{Nb5+} = 0.66 Å, r_{Ta5+} = 0.66 Å), therefore we can discuss the metrical properties of Ta–O by comparing them with those of Nb–O. The distances of Ta–O and Nb–O vary greatly with different compounds and different coordination environments. As in $TiNb_{24}O_{62}$ (*7*), the octahedral interatomic distances of Nb–O vary widely between 2.41(6) and 1.72(6) Å, the tetrahedral distances between niobium and oxygen are 1.65(5) and 1.70(5), while in $SnTa_2O_7$ (*8*), the bond lengths of Ta–O are between 1.80(15) and 2.21(16) Å. Besides, the bond length of Ta–$(O–O)^{2-}$ (Table IV) is near Nb–$(O–O)^{2-}$ (1.993–2.066 Å) in

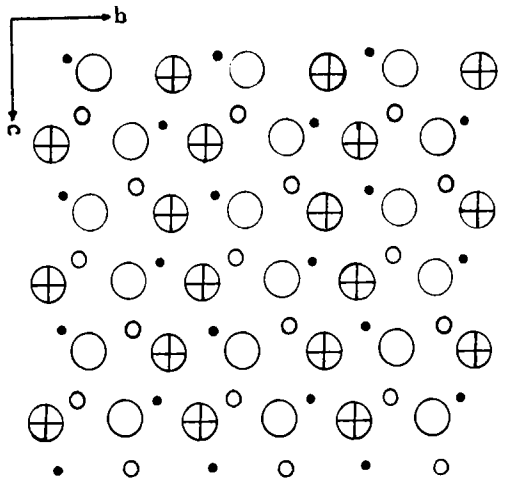

FIG. 1. Projection of three layers (bAc) onto the *b*–*c* plane: Ta atoms are small filled circles; *M* atoms are open circles; O(1) atoms are large crossed circles; O(2) atoms are large open circles.

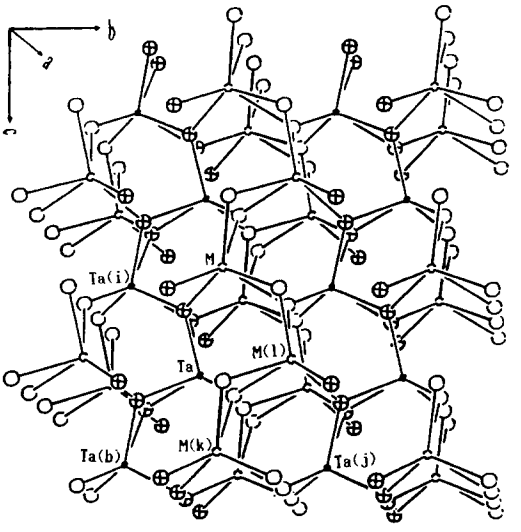

FIG. 2. Perspective view of the crystal structure of $[Fe_{0.3}Mn_{0.7}]Ta(O_2)O_2$ along [100]: Ta atoms are small filled circles; *M* atoms are small open circles.

TABLE IV

BOND DISTANCES (Å) AND ANGLES (deg.) FOR CRYSTAL OF $[Fe_{0.3}Mn_{0.7}]Ta(O_2)O_2$

Atom 1	Atom 2	Distance	Atom 1	Atom 2	Distance	Atom 1	Atom 2	Distance
O(1)	O(1*a*)	1.57(3)	O(1)	O(2)	2.84(1)	O(1*a*)	O(1*b*)	2.76(2)
O(1*c*)	O(2)	2.77(1)	O(1)	O(2*e*)	2.97(2)	O(1)	O(2*h*)	3.01(1)
O(1)	O(1*d*)	3.15(3)	O(2)	O(2*a*)	2.28(1)	O(2*e*)	O(2*h*)	2.86(3)
O(2*e*)	O(2*f*)	2.44(1)	Ta	O(1)	1.885(8)	Ta	O(1*b*)	1.995(9)
Ta	O(2)	1.74(2)	*M*	O(2*e*)	2.24(2)	*M*	O(2*g*)	2.10(2)
M	O(1)	2.206(7)	Ta	Ta(*i*)	3.22(1)	Ta	Ta(*j*)	4.41(3)
M	*M*(*k*)	3.16(3)						

Atom 1	Atom 2	Atom 3	Angle	Atom 1	Atom 2	Atom 3	Angle
O(1)	Ta	O(1*a*)	49.5(2)	O(1)	Ta	O(1*b*)	110.3(4)
O(1)	Ta	O(1*c*)	91.0(4)	O(1)	Ta	O(2)	103.2(4)
O(1)	Ta	O(2*a*)	141.0(5)	O(1*b*)	Ta	O(1*c*)	46.5(2)
O(1*b*)	Ta	O(2*a*)	95.4(4)	O(1*b*)	Ta	O(2)	127.6(4)
O(2)	Ta	O(2*a*)	81.7(5)	O(1)	*M*	O(1*d*)	91.2(3)
O(1)	*M*	O(2*e*)	89.0(3)	O(1)	*M*	O(2*f*)	144.6(4)
O(1)	*M*	O(2*g*)	132.6(4)	O(1)	*M*	O(2*h*)	84.1(4)
O(2*e*)	*M*	O(2*f*)	71.2(5)	O(2*e*)	*M*	O(2*g*)	120.5(4)
O(2*e*)	*M*	O(2*h*)	82.6(4)	O(2*g*)	*M*	O(2*h*)	66.2(4)
Ta	O(1)	*M*	122.2(5)	Ta	O(1)	Ta(*i*)	112.3(3)
Ta(*i*)	O(1)	*M*	125.6(4)	Ta(*i*)	Ta	Ta(*b*)	100.75(2)
Ta	O(2)	*M*(*k*)	129.2(5)	Ta	O(2)	*M*(*l*)	133.9(6)
M(*k*)	O(2)	*M*(*l*)	93.6(5)				

Symmetry code

a: $[1 - x, y, z]$ *b*: $[1 - x, -y, z + \frac{1}{2}]$ *c*: $[x, -y, z + \frac{1}{2}]$
d: $[-x, y, z]$ *e*: $[x, y, z - 1]$ *f*: $[-x, y, z - 1]$
g: $[-x, 1 - y, z - \frac{1}{2}]$ *h*: $[x, 1 - y, z - \frac{1}{2}]$ *i*: $[1 - x, -y, z - \frac{1}{2}]$
j: $[1 - x, 1 - y, \frac{1}{2} + z]$ *k*: $[x, y, 1 + z]$ *l*: $[-x, 1 - y, \frac{1}{2} + z]$

$KMgNb(O_2)_4 \cdot 7H_2O$ (*9*). Therefore the distances between Ta and O (1.74(2) ~ 1.995(9) Å) in the title compound are consistent with similar interactions in the known materials. The metallic environment of each Ta atom in an individual layer of Ta atoms includes two nearest-neighbor Ta atoms and two more distant Ta atoms (Fig. 2). Among the Ta–Ta distances, the shortest is 3.22(1) (Table IV).

The Fe and Mn atoms are stastically inserted into the distorted trigonal prismatic holes formed by six oxygen atoms. The distances between *M* and O are consistent with similar interactions in the materials α-Fe_2O_3 (*10*) (Fe–O: 1.945–2.116 Å, distorted octahedral) and Mn_5O_8 (*11*) (Mn–O: 2.05–2.31 Å, distorted trigonal prism). The shortest distance between the stastical metal atoms is 3.16(4) Å.

The O–O distances listed in Table IV range from 1.57(1) to 3.01(2) Å. The distance 1.57 Å is the classical bond length (*12*) of $(O–O)^{2-}$. Such an O–O distance is very interesting. It has been found that the O–O distances in tantalum oxide are often unusually short. In $NaTa_3O_8$ the nonbonding O–O distance around 2.20 Å was discovered (*13*), while in the binary system of Ta_2O_5–WO_3, the O–O distance of 2.06(33) Å was much shorter (*14*). Khitrova *et al.* had noticed the phenomenon; in the work

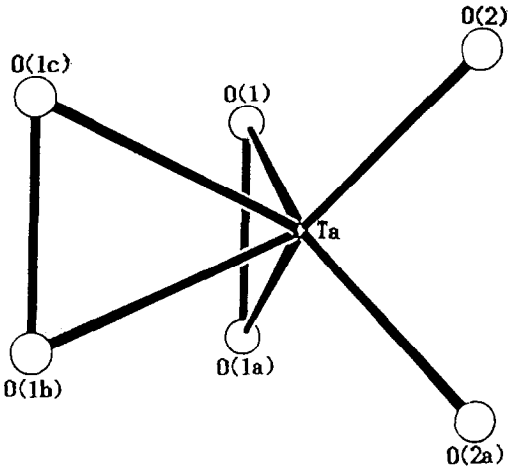

FIG. 3. The coordination polyhedron of the Ta atom.

on the structure of tantalum oxide they discovered the O–O "dumbell" (~1.3 Å) in δ'-Ta_2O_5 (*15*). Our work on single crystal structure determination of the title compound revealed clearly the existence of O–O bonding in the tantalum oxide system.

The O atoms are each bound to three metal atoms. The O · · · O distances between two nearest layers (perpendicular to the *a*-axis) are between 1.575–2.281 Å for (AbA) and 2.446–3.152 Å for (AcA), the latter are in the range of van der Waals' interactions observed in other materials: $TiNb_{24}O_{62}$ (*7*) (3.29 ~ 2.31 Å) and RMe_3O_9 (*16*) (2.92 ~ 2.65 Å) (*R* = rare earth or other trivalent metal, *Me* = Nb, Ta, or Pa). As the layers AbA are more closely packed than AcA, the structure may also be viewed as composed of $[Ta(O_2)O_2]^2_\infty$ layers with Fe and Mn inserted between these layers. All oxygen layers are directly superposed, with different O · · · O interaction distances, which also results in all the interstices being of distorted trigonal prisms, the packing is less regular and less efficient. The separate trigonal prismatic coordination polyhedrons of Ta atoms form the disconnected chains along the *a*-axis (Fig. 2), so it is different from that in MQ_3 (*M* = Nb, Ta; *Q* = S, Se) (*17*) and M_2PdQ_6 (*M* = Ta or Nb; *Q* = S or Se) (*18*), in which the trigonal-prismatic chains are continuous.

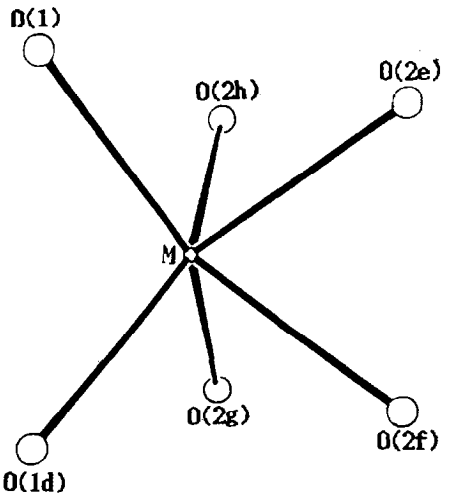

FIG. 4. The coordination polyhedron of the *M* atom.

The data of IR support the result of X-ray diffraction. The strong absorption peak around 870 cm^{-1} can be assigned to O–O streching vibrations (*19*). It is very difficult with certainty to assign ν_2 and ν_3 for bidentate peroxide groups (*19*), owing to the presence of strong broad absorption band between 500–800 cm^{-1}, in which other metal–oxygen, especially the Ta–O streching vibration, appear (*20, 21*).

From the simple structural nature of the title compound we may formulate an equally simple valence description of Fe^{II}, Mn^{II}, Ta^{IV}, $(O_2)^{-II}$, O^{-II}. With this formal valence description, the electronic levels of the atoms are energetically arranged in the increasing order O < Fe, Mn < Ta. If the metal atoms are considered to be $3d^6$Fe, $3d^5$Mn, and $5d^1$Ta, then at the Fermi level the dominating Ta character is anticipated. Of importance might be that the $5d^1$ electron could be used to force a weak metal–metal bond.

The results of electrical resistivity measurements on the crystal of $[Fe_{0.3}Mn_{0.7}]$

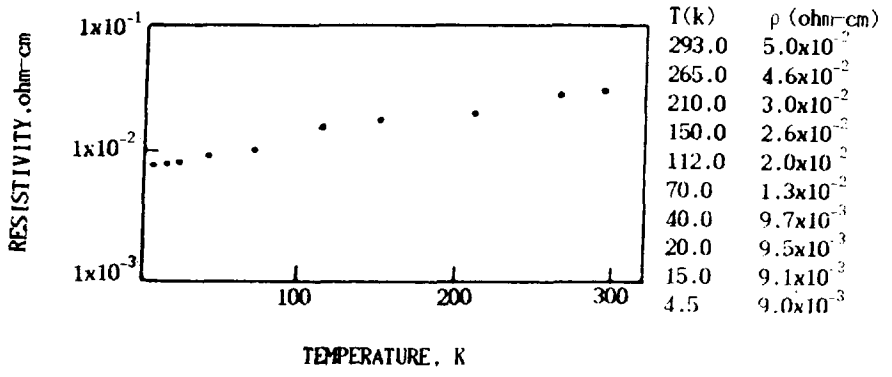

FIG. 5. Electrical resistivity in the c-direction vs temperature of the crystal of $[Fe_{0.3}Mn_{0.7}]Ta(O_2)O_2$.

$Ta(O_2)O_2$ are given in Fig. 5. The resistivity decreases slightly and shows no superconductivity of the new material in the range measured. It behaved typically as a saturated semiconductor. Considering the structure results and these limited transport data, the behavior may be attributed to the statistical occupation of the M site by Fe and Mn. In order to understand the properties of the material, we shall calculate the electronic structure of the title compound in the forthcoming work (*22*).

Acknowledgments

This research was supported by the National Natural Science Foundation of China. Professor Lu Shao-Fang is thanked for helpful discussions in determining the structure. Mr. Zhang Ying-Chao is thanked for measuring electrical resistivity. Mr. Chen Ze-Shu is thanked for elemental analysis. Mr. Yang Anyi of the Institute of Geochemistry, Chinese Academy of Sciences, is thanked for measuring the density and the oxygen content. Ms. Cheng Buo is thanked for IR experimental data.

References

1. A. F. WELLS, "Structural Inorganic Chemistry," 4th ed., p. 454, Oxford Univ. Press, Oxford (1975).
2. J. E. FAGEL, R. F. WITBECK, AND H. A. SMITH, *Anal. Chem.* **31,** 1115 (1959).
3. W. R. HANSEN AND M. W. MALLET, *Anal. Chem.* **29,** 1868 (1957).
4. H. C. MONTGOMERY, *J. Appl. Phys.* **42**(7), 2971 (1971).
5. D. E. SCHAFER *et al.*, *Solid State Commun.* **14,** 347 (1974).
6. B. K. VAINSHTEIN, V. M. FRIDKIN, AND V. L. INDENBOM, "Modern Crystallography II: Structure of Crystals," Springer Series in Solid-State Sciences, Vol. 21, pp. 71–81, Springer-Verlag, Berlin (1982).
7. R. S. ROTH AND A. D. WADSLEY, *Acta Crystallogr.* **18,** 724 (1965).
8. W. G. MUMME, *Am. Miner.* **155,** 367 (1970).
9. G. MATHERN AND R. WEISS, *Acta Crystallogr., Sect. B: Struct. Crystallogr. Cryst. Chem.* **27,** 1958 (1971).
10. A. F. WELLS, "Structural Inorganic Chemistry," 4th ed., p. 451, Oxford Univ. Press, Oxford (1975).
11. H. R. OSWALD AND M. J. WAMPETICH, *Helv. Chim. Acta* **50,** 2023 (1967).
12. A. F. WELLS, "Structural Inorganic Chemistry," 4th ed., p. 422, Oxford Univ. Press, Oxford (1975).
13. P. N. IYER AND A. J. SMITH, *Acta Crystallogr.* **23,** 740 (1967).
14. (a) J. RIJINSDORP AND F. J. JELLINEK, *J. Solid State Chem.* **25,** 325 (1978); (b) J. L. HODEAU AND M. MAREZIO, *J. Phys. C* **11,** 4117 (1978); (c) A. MEERSCHAUT AND L. GUEMAS, *J. Solid State Chem.* **36,** 118 (1981).
15. D. A. KESZLER *et al.*, *Inorg. Chem.* **24,** 3063 (1985).
16. K.-J RANGE, M. WILDENAUER, AND A. M. HEYNS, *Angew Chem. Int. Ed. Engl.* **27**(7), 969 (1988).
17. N. C. STEPHENSON AND R. S. ROTH, *Acta Crystallogr., Sect. B: Struct. Crystallogr. Cryst. Chem.* **27,** 1025 (1971).

18. V. I. KHITROVA AND V. V. KLECHKOVSKAYA, *Kristallografiya* **25**(6), 1169 (1980).
19. W. P. GRIFFITH AND T. D. WICKINGS, *J. Chem. Soc. A* 397 (1968).
20. R. A. NYQUIST AND R. O. KAGEL, "Infrared Spectra of Inorganic Compounds," Academic Press, New York and London (1971).
21. K. NAKAMOTO, "Infrared Spectra of Complex Molecules," Wiley, New York (1963).
22. HUANG JING-LING AND DENG SHUIQUAN, to be submitted.
23. R. C. G. KILLEAN AND J. L. LAWRENCE, *Acta Crystallogr.* **25,** 1750 (1969).